

Exponential Sum Approximations and Fast Evaluation of Fractional Integrals

William McLean

Abstract Given $\beta > 0$ and $\delta > 0$, the function $t^{-\beta}$ may be approximated for t in the interval $[\delta, 1]$ by a sum of terms of the form $w e^{-at}$, with parameters $w > 0$ and $a > 0$. A basic approximation is obtained by applying quadratures to an integral representation of $t^{-\beta}$. This basic approximation is then improved by solving a nonlinear optimization problem. In a third step, a new exponential sum approximation, with fewer terms but comparable accuracy, is constructed with the help of the eigenvalue decomposition of a certain symmetric positive-definite matrix. As an application, we describe a simple fast algorithm for computing a fractional integral at a sequence of grid points in the unit interval.

1 Introduction

Given $\beta > 0$ and $\delta > 0$, we consider approximations of the form

$$t^{-\beta} \approx \frac{1}{\Gamma(\beta)} \sum_{l=1}^L w_l e^{-a_l t} \quad \text{for } \delta \leq t \leq 1, \quad (1)$$

in which $0 < a_1 < a_2 < \dots < a_L$ and $w_l > 0$ for all l . Our aim is to achieve a desired maximum relative error tolerance $\varepsilon > 0$ while keeping the number of terms L small. It is natural to refer to the parameters w_l and a_l as the weights and nodes, respectively, because one approach to obtaining suitable values is to apply a quadrature rule to the integral representation

William McLean (✉)

School of Mathematics and Statistics, The University of New South Wales, Sydney 2052, AUSTRALIA

e-mail: w.mclean@unsw.edu.au

$$t^{-\beta} = \frac{1}{\Gamma(\beta)} \int_0^\infty e^{-tx} x^{\beta-1} dx, \quad t > 0. \quad (2)$$

For instance, Beylkin and Monzón [2] used the substitution $x = e^y$ to derive

$$t^{-\beta} = \frac{1}{\Gamma(\beta)} \int_{-\infty}^\infty \exp(-te^y + \beta y) dy \approx \frac{h}{\Gamma(\beta)} \sum_{n=-M+1}^N \exp(-te^{nh} + \beta nh), \quad (3)$$

which has the form (1) with

$$w_l = he^{\beta(l-M)} \quad \text{and} \quad a_l = e^{(l-M)h} \quad \text{for } 1 \leq l \leq L = M + N.$$

They showed [2, Theorem 5] that, taking $h = O(1/\log \varepsilon^{-1})$, it suffices to choose M of order $(\log \varepsilon^{-1})^2$ and N of order $(\log \varepsilon^{-1})(\log \log \varepsilon^{-1} + \log \delta^{-1})$ to ensure a relative error less than ε for $\delta \leq t \leq 1$.

Exponential sum approximations like (1) have been used in fast algorithms for evaluation of convolution integral operators with a variety of kernels. Braess and Hackbusch [3, 4] considered approximations to $1/x$ for $1 \leq x < \infty$. In connection with the use of nonreflecting boundary conditions for the wave equation, Alpert, Greengard and Hagstrom [1] approximated the inverse Laplace transform of the logarithmic derivative of a Hankel function using exponential sums with complex weights and nodes. Xu and Jiang [13] discuss several kernels, including those arising in the Havriliak–Negami dielectric model and in nonreflecting boundary conditions for the Schrödinger equation.

Here we take as an application the problem of computing a fractional integral of order α ,

$$I^\alpha u(t) = \int_0^t \frac{(t-s)^{\alpha-1}}{\Gamma(\alpha)} u(s) ds, \quad t > 0, \quad (4)$$

at discrete grid points $0 = t_0 < t_1 < t_2 < \dots < t_N = 1$, assuming $0 < \alpha < 1$. If, for simplicity, u is approximated by a piecewise-constant function

$$U(t) = U^j \quad \text{for } t_{j-1} < t < t_j,$$

with $U^j \approx u(t_j)$, then

$$I^\alpha u(t_n) \approx I^\alpha U(t_n) = \sum_{j=1}^n \omega_{nj} U^j \quad \text{for } 1 \leq n \leq N, \quad (5)$$

where the weights in the sum are given by

$$\omega_{nj} = \int_{t_{j-1}}^{t_j} \frac{(t_n - s)^{\alpha-1}}{\Gamma(\alpha)} ds = \frac{(t_n - t_{j-1})^\alpha - (t_n - t_j)^\alpha}{\Gamma(1 + \alpha)} > 0. \quad (6)$$

Direct evaluation of the N sums in (5) costs $\sum_{n=1}^N n \approx N^2/2$ operations.

Now fix $p \geq 1$. The exponential sum approximation (1), with $\beta = 1 - \alpha$, allows us to write, for $n \geq p$ and $t_n - t_{n-p} \geq \delta$,

$$\begin{aligned} \sum_{j=1}^{n-p} \omega_{nj} U^j &= \int_0^{t_{n-p}} \frac{(t_n - s)^{\alpha-1}}{\Gamma(\alpha)} U(s) ds \\ &\approx \frac{1}{\Gamma(\alpha)\Gamma(1-\alpha)} \int_0^{t_{n-p}} \sum_{l=1}^L w_l e^{-a_l(t_n-s)} U(s) ds, \end{aligned} \quad (7)$$

so, in light of the identity $\Gamma(\alpha)\Gamma(1-\alpha) = \pi/\sin\pi\alpha$,

$$\sum_{j=1}^{n-p} \omega_{nj} U^j \approx \frac{\sin\pi\alpha}{\pi} \sum_{l=1}^L \Theta_l^n \quad \text{where} \quad \Theta_l^n = \int_0^{t_{n-p}} w_l e^{-a_l(t_n-s)} U(s) ds.$$

Putting $\Delta t_n = t_n - t_{n-1}$, we find that $\Theta_l^n = \sum_{j=1}^{n-p} \kappa_{lnj} U^j$, where

$$\kappa_{lnj} = \int_{t_{j-1}}^{t_j} w_l e^{-a_l(t_n-s)} ds = \frac{w_l}{a_l} e^{-a_l(t_n-t_j)} (1 - e^{-a_l\Delta t_j}).$$

The approximate representation

$$I^\alpha U(t_n) \approx I_{L,p}^\alpha U(t_n) \equiv \frac{\sin\pi\alpha}{\pi} \sum_{l=1}^L \Theta_l^n + \sum_{j=n-p+1}^n \omega_{nj} U^j \quad (8)$$

has the advantage that the Θ_l^n can be computed via the recurrence relation

$$\Theta_l^n = \kappa_{ln,n-p} U^{n-p} + e^{-a_l\Delta t_n} \Theta_l^{n-1} \quad \text{for } n \geq p+1, \text{ with } \Theta_l^p = 0. \quad (9)$$

In this way, we may (approximately) evaluate $I^\alpha U(t_n)$ for $1 \leq n \leq N$ with $N(L+p)$ operations, which is a substantial saving provided $L+p \ll N$. Jiang et al. [6] describe a similar fast algorithm for evaluating a (Caputo) fractional *derivative*. Practically speaking, these fast algorithms are useful if U^j is not a scalar but a large vector, as occurs when solving fractional PDEs. In this context, the simplicity of the approach is attractive in comparison to alternative fast methods [9, 10, 11], particularly when using non-uniform time steps.

The approximation (1) for $t \in [\delta, 1]$ can be rescaled to the interval $[\delta \cdot T, T]$ for any $T > 0$. Indeed, since

$$t^{-\beta} = T^{-\beta} \left(\frac{t}{T}\right)^{-\beta} \approx \frac{T^{-\beta}}{\Gamma(\beta)} \sum_{l=1}^L w_l e^{-a_l t/T} \quad \text{for } \delta \leq \frac{t}{T} \leq 1,$$

if we put $\check{w}_l = w_l/T^\beta$ and $\check{a}_l = a_l/T$, then

$$t^{-\beta} \approx \frac{1}{\Gamma(\beta)} \sum_{l=1}^L \check{w}_l e^{-\check{a}_l t} \quad \text{for } \delta \cdot T \leq t \leq T. \quad (10)$$

One easily verifies that the maximum relative error is the same for both (1) and (10). Also, the fast evaluation scheme (8) discussed above easily generalizes to allow grid

points in the interval $[0, T]$. For the simple case when $p = 1$ and the N grid points are uniformly spaced, we require $\delta \leq \Delta t/T = 1/N$ so that, cf. (7),

$$\delta \cdot T \leq t_n - s \leq T \quad \text{for } 0 \leq s \leq t_{n-1}.$$

In Section 2, we derive an exponential sum approximation (1) based, not on the quadrature rule (3), but on the approach of Jiang et al. [6] using composite Gauss quadrature over dyadic intervals. We present a simplified error analysis showing that the relative error can be held below ε with the number of terms L of order $(\log \varepsilon^{-1}) \log(\delta^{-1} \log \varepsilon^{-1})$. A somewhat different approach to fast evaluation of fractional integrals was earlier given by Li [9], involving a quadrature approximation with order $\log(\varepsilon^{-1} \delta^{-1})^2$ terms, but which is valid for $\delta \leq t < \infty$.

Section 3 describes how we can attempt to improve the accuracy of any exponential sum approximation to $t^{-\beta}$ by solving a nonlinear, constrained optimization problem. Next, in Section 4, we explain how a given exponential sum can be approximated by one with fewer terms, where the accuracy depends on the decay of the eigenvalues of the $L \times L$ matrix $[\sqrt{w_i} \sqrt{w_j} / (a_i + a_j)]$. This procedure is a special case of a model reduction technique used in control theory [5, 13]. We provide illustrative numerical examples throughout Sections 2–4, and conclude the paper, in Section 5 with some further computational experiments.

2 Gauss quadrature over dyadic intervals

Following Jiang et al. [6], we split the integral in (2) as follows,

$$\frac{1}{t^\beta} = \frac{1}{\Gamma(\beta)} \left(\int_0^2 + \int_2^4 + \int_4^8 + \cdots + \int_{2^{J-1}}^{2^J} + \int_{2^J}^{\infty} \right) e^{-ty} y^{\beta-1} dy,$$

and separately approximate each of the $J + 1$ integrals on the right-hand side using Gauss quadrature, except for the integral over $(2^J, \infty)$, which can be bounded in terms of the upper incomplete Gamma function,

$$\Gamma(\beta, z) = \int_z^{\infty} e^{-s} s^{\beta-1} ds.$$

Lemma 1. *Let $\Delta_J = \Gamma(\beta, \delta 2^J) / \Gamma(\beta)$. Then*

$$0 \leq \frac{1}{\Gamma(\beta)} \int_{2^J}^{\infty} e^{-ty} y^{\beta-1} dy \leq \Delta_J t^{-\beta} \quad \text{for } \delta \leq t \leq 1.$$

Proof. The substitution $y = x/t$ gives

$$\frac{t^\beta}{\Gamma(\beta)} \int_{2^J}^{\infty} e^{-ty} y^{\beta-1} dy = \frac{1}{\Gamma(\beta)} \int_{t2^J}^{\infty} e^{-x} x^{\beta-1} dx = \frac{\Gamma(\beta, t2^J)}{\Gamma(\beta)}, \quad (11)$$

and $\Gamma(\beta, t2^J)$ is a decreasing function of t . \square

To approximate the integral over $[0, 2]$, we use a Gauss–Jacobi rule,

$$\int_{-1}^1 f(s)(s+1)^{\beta-1} ds = \sum_{n=1}^{\tilde{N}} \tilde{W}_n f(\tilde{S}_n) + \tilde{E}_{\tilde{N}}(f), \quad (12)$$

noting that the weights \tilde{W}_n and nodes \tilde{S}_n depend on \tilde{N} and β . The next theorem provides a derivative-free bound for the error term $\tilde{E}_{\tilde{N}}(f)$. For $b > 0$ and $\rho = e^b > 1$, the equation to the *Bernstein ellipse* \mathcal{E}_ρ in the complex z -plane is

$$\frac{(\Re z)^2}{\cosh^2 b} + \frac{(\Im z)^2}{\sinh^2 b} = 1,$$

and we note that $\rho = \cosh b + \sinh b$ is the sum of the semimajor and semiminor axes.

Theorem 1. *If $f(z)$ is analytic in a convex open set containing the Bernstein ellipse \mathcal{E}_ρ , and if*

$$|f(z)| \leq M_\rho \quad \text{for all } z \in \mathcal{E}_\rho,$$

then

$$|\tilde{E}_{\tilde{N}}(f)| \leq \frac{2^{\beta+2} M_\rho}{\beta} \frac{\rho^{-2\tilde{N}}}{1 - \rho^{-2}} \quad \text{for } \tilde{N} \geq 1.$$

Proof. Since $4 \int_{-1}^1 (s+1)^{\beta-1} ds = 2^{\beta+2}/\beta$, the estimate follows by a result of von Sydow [12, Theorem 1]. \square

The change of variable $y = s + 1$ yields the desired bound.

Lemma 2. *If $0 \leq t \leq 1$, then*

$$\left| \frac{1}{\Gamma(\beta)} \int_0^2 e^{-ty} y^{\beta-1} dy - \frac{1}{\Gamma(\beta)} \sum_{n=1}^{\tilde{N}} \tilde{W}_n e^{-\tilde{Y}_n t} \right| \leq \tilde{R}_{\tilde{N}} t^{-\beta},$$

where

$$\tilde{Y}_n = \tilde{S}_n + 1 \quad \text{and} \quad \tilde{R}_{\tilde{N}} = \frac{2^{\beta+2}}{\Gamma(\beta+1)} e^{\cosh b - 1} \frac{\rho^{-2\tilde{N}}}{1 - \rho^{-2}}.$$

Proof. Define the entire function $f(z) = e^{-t(z+1)}/\Gamma(\beta)$. Since

$$\frac{1}{\Gamma(\beta)} \int_0^2 e^{-ty} y^{\beta-1} dy = \int_{-1}^1 f(s)(s+1)^{\beta-1} ds,$$

and $-\cosh b \leq \Re z \leq \cosh b$ for $z \in \mathcal{E}_\rho$, we may take $M_\rho = e^{t(\cosh b - 1)}/\Gamma(\beta)$ in Theorem 1 and obtain

$$t^\beta |\tilde{E}_{\tilde{N}}| \leq \frac{2^{\beta+2}}{\Gamma(\beta+1)} t^\beta e^{(\cosh b - 1)t} \frac{\rho^{-2\tilde{N}}}{1 - \rho^{-2}}. \quad (13)$$

Since $t^\beta e^{(\cosh b - 1)t} \leq e^{\cosh b - 1}$ for $0 \leq t \leq 1$, the estimate for \tilde{R}_N follows. \square

We approximate the integral over $[2^{j-1}, 2^j]$ using a Gauss–Legendre rule,

$$\int_{-1}^1 f(s) ds = \sum_{p=1}^N W_p f(S_p) + E_N(f),$$

which is just the special case $\beta = 1$ of (12), so by Theorem 1,

$$|E_N(f)| \leq 8M_\rho \frac{\rho^{-2N}}{1 - \rho^{-2}}. \quad (14)$$

This time, the required change of variable is $y = 2^{j-2}(s+3)$ for $-1 \leq s \leq 1$.

Lemma 3. Let $0 < \nu < 2$, define $b > 0$ by $\cosh b = 3 - \nu$ and put

$$\rho = e^b = 3 - \nu + \sqrt{(2 - \nu)(4 - \nu)} > 1. \quad (15)$$

Then

$$\left| \frac{1}{\Gamma(\beta)} \int_{2^{j-1}}^{2^j} e^{-ty} y^{\beta-1} dy - \frac{2^{j-2}}{\Gamma(\beta)} \sum_{n=1}^N W_n Y_{jn}^{\beta-1} e^{-tY_{jn}} \right| \leq R_N t^{-\beta}$$

where $Y_{jn} = 2^{j-2}(S_n + 3)$ and

$$R_N = \frac{8}{\Gamma(\beta)} \left(\frac{\beta}{e\nu} \right)^\beta \frac{\rho^{-2N}}{1 - \rho^{-2}} \times \begin{cases} \nu^{\beta-1}, & 0 < \beta \leq 1, \\ (6 - \nu)^{\beta-1}, & \beta > 1. \end{cases}$$

Proof. Letting $y(z) = 2^{j-2}(z+3)$ we have

$$\frac{1}{\Gamma(\beta)} \int_{2^{j-1}}^{2^j} e^{-ty} y^{\beta-1} dy = \int_{-1}^1 f(s) ds,$$

where the function

$$f(z) = \frac{2^{j-2}}{\Gamma(\beta)} e^{-ty(z)} y(z)^{\beta-1} = \frac{2^{\beta(j-2)}}{\Gamma(\beta)} (z+3)^{\beta-1} \exp(-t2^{j-2}(z+3))$$

is analytic for $z \notin (-\infty, -3]$, with

$$\Re(z+3) \geq \nu \quad \text{and} \quad \nu \leq |z+3| \leq 6 - \nu \quad \text{for } z \in \mathcal{E}_\rho.$$

Thus, we may apply (14) with

$$M_\rho = \frac{2^{\beta(j-2)}}{\Gamma(\beta)} \exp(-t2^{j-2}\nu) \times \begin{cases} \nu^{\beta-1}, & 0 < \beta \leq 1, \\ (6 - \nu)^{\beta-1}, & \beta > 1, \end{cases}$$

and put $g(x) = x^\beta e^{-x}$ to arrive at the estimate

$$t^\beta |E_N(f)| \leq \frac{8}{\Gamma(\beta)} \frac{g(t2^{j-2}\nu)}{\nu^\beta} \frac{\rho^{-2N}}{1-\rho^{-2}} \times \begin{cases} \nu^{\beta-1}, & 0 < \beta \leq 1, \\ (6-\nu)^{\beta-1}, & \beta > 1. \end{cases} \quad (16)$$

Since $0 < g(x) \leq g(\beta) = \beta^\beta e^{-\beta}$ for $0 < x < \infty$, the desired estimate follows at once. \square

Given $\varepsilon > 0$, we choose first J , followed by \tilde{N} and N , such that

$$\Delta_J \leq \frac{\varepsilon}{J+1}, \quad |\tilde{R}_{\tilde{N}}| \leq \frac{\varepsilon}{J+1}, \quad |R_N| \leq \frac{\varepsilon}{J+1}, \quad (17)$$

and define the weights w_l and nodes a_l by

$$\sum_{l=1}^L w_l e^{-a_l t} = \sum_{n=1}^{\tilde{N}} \tilde{W}_n e^{-\tilde{Y}_n t} + \sum_{j=2}^J 2^{j-2} \sum_{n=1}^N W_n Y_{jn}^{\beta-1} e^{-Y_{jn} t}. \quad (18)$$

In this way,

$$\left| t^{-\beta} - \frac{1}{\Gamma(\beta)} \sum_{l=1}^L w_l e^{-a_l t} \right| \leq \varepsilon t^{-\beta} \quad \text{for } \delta \leq t \leq 1,$$

with

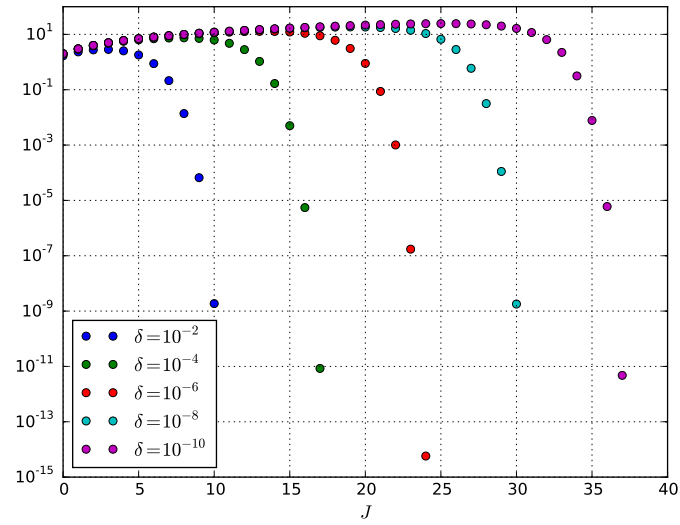
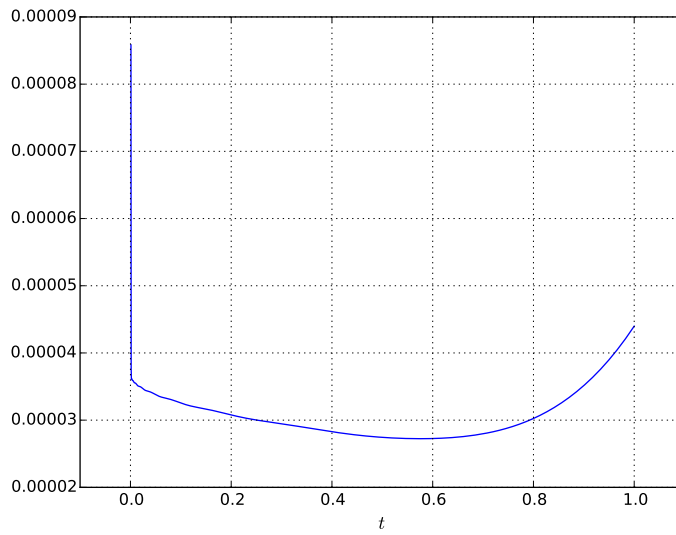
$$J = O(\log(\delta^{-1} \log \varepsilon^{-1})), \quad \tilde{N} = O(\log \varepsilon^{-1}), \quad N = O(\log \varepsilon^{-1}).$$

Hence, $L = \tilde{N} + (J-1)N$ is of order $(\log \varepsilon^{-1}) \log(\delta^{-1} \log \varepsilon^{-1})$.

Table 1 Decay of $\tilde{R}_{\tilde{N}}$ and R_N with optimal choices of b .

$\tilde{N} = N$	$\tilde{R}_{\tilde{N}}$	b	R_N	b
2	3.38e-02	2.1020	7.64e-03	1.5461
4	1.69e-06	2.7774	1.24e-05	1.6465
6	1.07e-11	3.1801	1.57e-08	1.6834
8	1.75e-17	3.4668	1.79e-11	1.7025
10	1.05e-23	3.6896	1.93e-14	1.7142
12	2.81e-30	3.8717	2.00e-17	1.7221

Example 1. Figure 1 illustrates the decay behaviour of $(J+1)\Delta_J$ when $\beta = 1/2$, for different choices of δ . Table 1 shows the decay of the error bounds $\tilde{R}_{\tilde{N}}$ and R_N , along with the values of the parameter b used. The latter were chosen to minimise the error bound in each case. With $\delta = 10^{-3}$ and $\varepsilon = 10^{-2}$, we find that $J = 13$, $\tilde{N} = 3$ and $N = 3$ are the smallest choices for which (17) holds, giving a total of $L = 39$ terms. Using these values in (18), the maximum relative error is in fact much smaller than ε , as shown in Figure 2, although the relative error spikes near $t = \delta$. This behaviour becomes more extreme if we reduce δ or ε , and the spike is not surprising given the dependence on t seen in (11) and (16). We observed that computing J , \tilde{N} and N for the interval $[\delta/2, 1]$ has the effect of eliminating the spike near $t = \delta$ in the

Fig. 1 Decay of $(J+1)\Delta_J$ when $\beta = 1/2$.**Fig. 2** Relative error when $J = 13$, $\tilde{N} = 3$ and $N = 3$.

interval $[\delta, 1]$. For the present example, doing so gives the new value $J = 14$, with $\tilde{N} = 3$ and $N = 3$ unchanged, leading to an additional three terms in the exponential sum (that is, $L = 42$). The plot of the relative error is then indistinguishable from Figure 2 except for the absence of the spike at $t = \delta$.

3 Optimizing the weights and nodes

Ideally, for a given L we would like to find the best possible vectors of weights $\mathbf{w} = (w_1, w_2, \dots, w_L)$ and nodes $\mathbf{a} = (a_1, a_2, \dots, a_L)$, in the sense of minimizing the relative error in the exponential sum approximation (1). In other words, we would like to solve the minimax optimization problem

$$\min_{w_l \geq 0, a_l \geq 0} \max_{\delta \leq t \leq 1} \left| 1 - \frac{t^\beta}{\Gamma(\beta)} \sum_{l=1}^L w_l e^{-a_l t} \right|.$$

More realistically, we can replace the continuous maximum by the maximum over some discrete grid points

$$\delta = t_1 < t_2 < t_3 < \dots < t_Q = 1 \quad (19)$$

and define $f_q : \mathbb{R}^{2P} \rightarrow \mathbb{R}$ by

$$f_q(\mathbf{x}) = 1 - \frac{t_q^\beta}{\Gamma(\beta)} \sum_{l=1}^L w_l e^{-a_l t_q}, \quad 1 \leq q \leq Q,$$

where

$$\mathbf{x} = (a_1, w_1, a_2, w_2, \dots, a_L, w_L). \quad (20)$$

Our optimization problem using the points (19) then becomes

$$\min_{x_j \geq 0} \max_{1 \leq q \leq Q} |f_q(\mathbf{x})|.$$

Since $\max_q |f_q(\mathbf{x})|$ is not differentiable, we introduce an additional variable y and instead consider the equivalent problem

$$\min_{(\mathbf{x}, y) \in S} y$$

where the feasible set $S \subseteq \mathbb{R}^{2L+1}$ is defined by the nonlinear (but smooth) constraints

$$-y \leq f_q(\mathbf{x}) \leq y \quad \text{for } 1 \leq q \leq Q, \quad (21)$$

together with the lower bounds

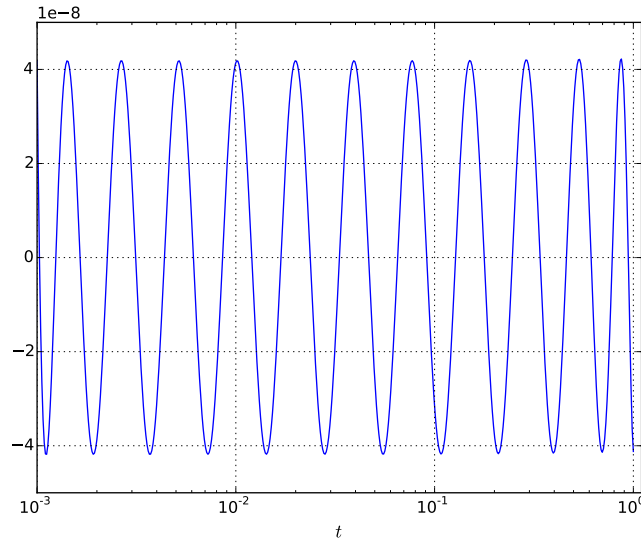
$$x_j \geq 0 \text{ for } 1 \leq j \leq 2L \quad \text{and} \quad y \geq 0.$$

In this way, $|f_q(\mathbf{x})| \leq y$ so

$$\left| t_q^{-\beta} - \frac{1}{\Gamma(\beta)} \sum_{l=1}^L w_l e^{-a_l t_q} \right| \leq y t_q^{-\beta} \quad \text{for } 1 \leq q \leq Q,$$

and, if necessary, we can relabel the weights and nodes so that the latter form an increasing sequence.

Fig. 3 Relative error using optimized nodes and weights.



Example 2. Once again, we let $\beta = 1/2$ and $\delta = 10^{-3}$. For points (19) of the form

$$t_q = 10^{-r(Q-q)/(Q-1)}$$

with $Q = 500$ and $r = 3$ (so $\delta = 10^{-r}$), we used a sequential least-squares, quadratic programming method of Kraft [8], accessed as the option `:LD_SLSQP` in the Julia bindings (`NLOpt.jl`) for the nonlinear optimization package of Johnson [7]. As the starting value for \mathbf{x} in (20), we chose the $L = 42$ spike-free nodes a_l and weights w_l from Example 1 (that is, with $J = 14$ and $\tilde{N} = N = 3$), and as the starting value for y we chose $\max_{1 \leq q \leq Q} |f_q(\mathbf{x})|$. After 2,236 iterations, the optimization routine returned new nodes and weights, for which the relative error was as shown in Figure 3. Comparison with Figure 2 reveals that the optimization process reduced the maximum relative error from about 4.4×10^{-5} to about 4.2×10^{-8} . Figure 3 also shows why it is necessary to use a large number of points t_q clustered near δ ; note

the logarithmic scale on the t axis. Otherwise, if the spacing is too wide, the relative error spikes between successive t_q when q is small. The optimization routine takes about 13 seconds on a desktop PC with an Intel Core i7-4770 CPU (3.40 GHz).

4 Reducing the number of terms

The feasible set S for the constraints (21) is not convex so, from our chosen initial value of (\mathbf{x}, y) , the optimization routine will most likely converge to a nearby local minimum, and not to a global minimum. Instead of trying to minimize the relative error for a fixed number of terms L , we now attempt to reduce the number of terms for a (roughly) fixed relative accuracy. We might hope that the resulting exponential sum is close to being globally optimal for this reduced number of terms. The following approach is based on a sum-of-poles approximation method of Xu and Jiang [13] used by Jiang et al. [6, Remark 4].

For a given function $g(t)$, let us write

$$G(z) = \int_{-\infty}^{\infty} e^{-zt} g(t) dt,$$

so that $y \mapsto G(iy)$ is the Fourier transform of g , and if $g(t) = 0$ for $t < 0$ then $G(z)$ is the Laplace transform of g . Consider g of the form

$$g(t) = \begin{cases} 0, & t < 0, \\ \sum_{l=1}^L w_l e^{-a_l t}, & t \geq 0, \end{cases}$$

and observe that the Laplace transform is a sum of poles,

$$G(z) = \sum_{l=1}^L \frac{w_l}{z + a_l}.$$

We will assume $a_l > 0$ and $w_l > 0$ for all l . By defining

$$A = \begin{bmatrix} a_1 & & & \\ & a_2 & & \\ & & \ddots & \\ & & & a_L \end{bmatrix} \in \mathbb{R}^{L \times L} \quad \text{and} \quad B = \begin{bmatrix} \sqrt{w_1} \\ \sqrt{w_2} \\ \vdots \\ \sqrt{w_L} \end{bmatrix} \in \mathbb{R}^{L \times 1}, \quad (22)$$

we can write

$$g(t) = B^T e^{-tA} B \quad \text{for } t \geq 0,$$

and

$$G(z) = B^T (zI + A)^{-1} B.$$

In the language of control theory, $G(z)$ is the *transfer function* of the dynamical system

$$\frac{d\mathbf{x}}{dt} + A\mathbf{x} = Bu(t), \quad y = B^T \mathbf{x},$$

with (scalar) control $u(t)$ and (scalar) output $y(t)$. That is, the relation between the transforms of the control and the output is given by $Y(z) = G(z)U(z)$. We can therefore apply a known model reduction technique [5] to obtain a sum with fewer than L terms. The process is simplified in our case because A is real, symmetric and positive-definite (even diagonal), and because the matrix B^T (in this case, a row vector) appearing in the output equation coincides with the transpose of the matrix B (in this case, a column vector) appearing in the forcing term of the ODE.

The *controllability gramian* is the matrix $P \in \mathbb{R}^{L \times L}$ defined by

$$P = \int_0^\infty e^{-tA} B B^T e^{-tA} dt, \quad (23)$$

which in our case coincides with the *observability gramian*, and satisfies the *Lya-punov equation*

$$AP + PA = [-e^{-tA} B B^T e^{-tA}]_0^\infty = B B^T.$$

It follows easily that the entries of P are

$$p_{ij} = \frac{b_i b_j}{a_i + a_j} = \frac{\sqrt{w_i} \sqrt{w_j}}{a_i + a_j}. \quad (24)$$

The Hankel operator $\mathcal{G} : L_2(\mathbb{R}_-) \rightarrow L_2(\mathbb{R}_+)$ is defined by

$$\mathcal{G}v(t) = \int_{-\infty}^0 g(t-s)v(s) ds \quad \text{for } 0 < t < \infty,$$

so that if the control satisfies $u(t) = 0$ for $t > 0$, then the output is $y(t) = \mathcal{G}u(t)$. The adjoint of the Hankel operator, $\mathcal{G}^* : L_2(\mathbb{R}_+) \rightarrow L_2(\mathbb{R}_-)$, is given by

$$\mathcal{G}^*v(t) = \int_0^\infty g(s-t)v(t) ds \quad \text{for } -\infty < t < 0.$$

Let $\boldsymbol{\eta}_1, \boldsymbol{\eta}_2, \dots, \boldsymbol{\eta}_L$ be an orthonormal basis for \mathbb{R}^L consisting of eigenvectors of the symmetric positive-definite matrix P , ordered so that the corresponding eigenvalues satisfy

$$\sigma_1 \geq \sigma_2 \geq \dots \geq \sigma_L > 0;$$

thus,

$$P\boldsymbol{\eta}_l = \sigma_l \boldsymbol{\eta}_l \quad \text{with} \quad \boldsymbol{\eta}_j^T \boldsymbol{\eta}_l = \delta_{jl}.$$

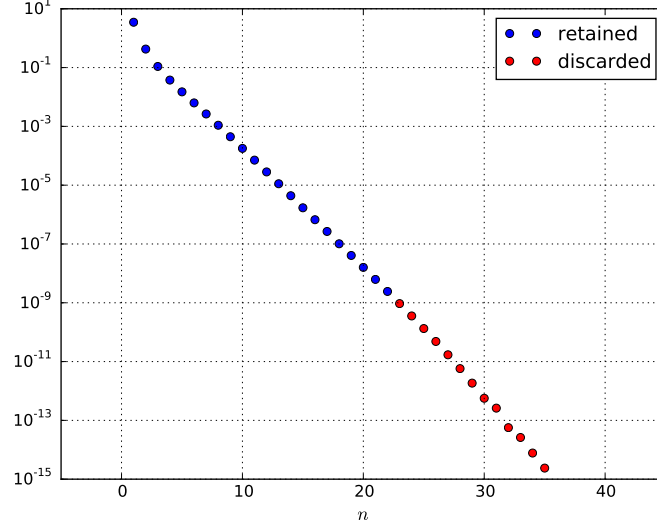
Define

$$\phi_l(t) = \sigma_l^{-1/2} B^T e^{tA} \boldsymbol{\eta}_l \quad \text{for } t < 0,$$

and

$$\psi_l(t) = \sigma_l^{-1/2} B^T e^{-tA} \boldsymbol{\eta}_l \quad \text{for } t > 0.$$

Fig. 4 Hankel singular values for the 42 optimized nodes and weights of Example 2. The last few singular values are zero to machine precision, and so cannot be shown.



Since $g(t-s) = B^T e^{-tA} e^{sA} B$, elementary calculations show that

$$\mathcal{G}\phi_l = \sigma_l \psi_l \quad \text{and} \quad \mathcal{G}^* \psi_l = \sigma_l \phi_l \quad \text{for } 1 \leq l \leq L,$$

so the σ_l are the singular values of \mathcal{G} . Moreover,

$$\langle \phi_j, \phi_l \rangle_{L_2(\mathbb{R}_-)} = \sigma_j^{-1/2} \sigma_l^{-1/2} \boldsymbol{\eta}_j^T P \boldsymbol{\eta}_l = \delta_{jl}$$

and likewise

$$\langle \psi_j, \psi_l \rangle_{L_2(\mathbb{R}_+)} = \sigma_j^{-1/2} \sigma_l^{-1/2} \boldsymbol{\eta}_j^T P \boldsymbol{\eta}_l = \delta_{jl}.$$

Thus,

$$\mathcal{G}v(t) = \sum_{l=1}^L \sigma_l \langle v, \phi_l \rangle_{L_2(\mathbb{R}_-)} \psi_l(t) \quad \text{for } t > 0,$$

and

$$\mathcal{G}^* v(t) = \sum_{l=1}^L \sigma_l \langle v, \psi_l \rangle_{L_2(\mathbb{R}_+)} \phi_l(t) \quad \text{for } t < 0.$$

It follows that

$$g(t-s) = \sum_{l=1}^L \sigma_l \psi_l(t) \phi_l(s) \quad \text{for } -\infty < s < 0 < t < \infty.$$

Put

$$H = [\boldsymbol{\eta}_1 \ \boldsymbol{\eta}_2 \ \cdots \ \boldsymbol{\eta}_L] \in \mathbb{R}^{L \times L} \quad \text{and} \quad \Sigma = \begin{bmatrix} \sigma_1 & & & \\ & \sigma_2 & & \\ & & \ddots & \\ & & & \sigma_L \end{bmatrix} \in \mathbb{R}^{L \times L},$$

giving the eigenvalue decomposition $P = H\Sigma H^T$, and for $1 \leq m \leq L$ put

$$H_m = [\boldsymbol{\eta}_1 \ \boldsymbol{\eta}_2 \ \cdots \ \boldsymbol{\eta}_m] \in \mathbb{R}^{L \times m} \quad \text{and} \quad \Sigma_m = \begin{bmatrix} \sigma_1 & & & \\ & \sigma_2 & & \\ & & \ddots & \\ & & & \sigma_m \end{bmatrix} \in \mathbb{R}^{m \times m}.$$

We then define

$$A_m = H_m^T A H_m \in \mathbb{R}^{m \times m} \quad \text{and} \quad B_m = H_m^T B \in \mathbb{R}^m,$$

with the corresponding reduced kernel

$$g_m(t) = B_m^T e^{-tA_m} B_m \quad \text{for } t \geq 0,$$

and transfer function

$$G_m(z) = B_m^T (zI + A_m)^{-1} B_m.$$

We easily verify that the matrix $P_m = H_m^T P H_m \in \mathbb{R}^{m \times m}$ satisfies the Lyapunov equation

$$A_m P_m + P_m A_m = B_m B_m^T. \quad (25)$$

Since A_m is symmetric and positive definite, it has an eigenvalue decomposition $A_m = X \hat{A} X^T$, where $X \in \mathbb{R}^{m \times m}$ is orthogonal and

$$\hat{A} = X^T A_m X = \text{diag}(\hat{a}_1, \hat{a}_2, \dots, \hat{a}_m),$$

that is, $\hat{a}_n > 0$ denotes the n th eigenvalue of A_m . The matrix $\hat{P} = X^T P_m X \in \mathbb{R}^{m \times m}$ is a solution of

$$\hat{A} \hat{P} + \hat{P} \hat{A} = \hat{B} \hat{B}^T \quad \text{where} \quad \hat{B} = X^T B_m \in \mathbb{R}^m, \quad (26)$$

if and only if P_m is a solution of (25), and since \hat{A} is diagonal we see, as before in (24), that

$$\hat{p}_{ij} = \frac{\hat{b}_i \hat{b}_j}{\hat{a}_i + \hat{a}_j}.$$

Therefore \hat{P} is uniquely determined by (26), and hence P_m is uniquely determined by (25), proving that P_m is the reduced gramian, that is,

$$P_m = \int_0^\infty e^{-tA_m} B_m B_m^T e^{-tA_m} dt.$$

The transfer function is invariant under the change of basis given by X , that is, if we define

$$\hat{G}(z) = \hat{B}^T (zI + \hat{A})^{-1} \hat{B},$$

then $\hat{G}(z) = B_m^T X (zI + X^T A_m X)^{-1} X^T B_m = B_m^T (zI + A_m)^{-1} B_m = G_m(z)$. Likewise for the kernels of the corresponding Hankel operators, \mathcal{G} and \mathcal{G}_m ,

$$\hat{g}(t) = \hat{B}^T e^{-t\hat{A}} \hat{B} = B_m^T X e^{-tX^T A_m X} X^T B_m = B_m^T e^{-tA_m} B_m = g_m(t),$$

so if we put $\hat{w}_l = (\hat{b}_l)^2$ then

$$\hat{g}(t) = g_m(t) = \sum_{l=1}^m \hat{w}_l e^{-\hat{a}_l t}.$$

Since

$$H_m H_m^T \boldsymbol{\eta}_l = \begin{cases} \boldsymbol{\eta}_l, & 1 \leq l \leq m, \\ \mathbf{0}, & m+1 \leq l \leq N, \end{cases}$$

and $P_m(H_m^T \boldsymbol{\eta}_l) = H_m^T P H_m H_m^T \boldsymbol{\eta}_l$, we see that

$$P_m(H_m^T \boldsymbol{\eta}_l) = \begin{cases} \sigma_l(H_m^T \boldsymbol{\eta}_l), & 1 \leq l \leq m, \\ \mathbf{0}, & m+1 \leq l \leq L, \end{cases}$$

that is, $H_m^T \boldsymbol{\eta}_l$ is an eigenvector of P_m with eigenvalue σ_l if $l \leq m$. Thus, the singular values of the reduced Hankel operator \mathcal{G}_m equal the first m singular values of the original Hankel operator \mathcal{G} . Notice also that

$$(H_m^T \boldsymbol{\eta}_j)^T (H_m^T \boldsymbol{\eta}_l) = \boldsymbol{\eta}_j^T H_m H_m^T \boldsymbol{\eta}_l = \boldsymbol{\eta}_j^T \boldsymbol{\eta}_l = \delta_{jl} \quad \text{if } j, l \leq m.$$

It can be shown [5] that the operator norm of $\mathcal{G} - \mathcal{G}_m$ satisfies

$$\|\mathcal{G} - \mathcal{G}_m\|_{L_2(\mathbb{R}_-) \rightarrow L_2(\mathbb{R}_+)} = \sup_{-\infty < y < \infty} |G(iy) - \hat{G}(iy)| \leq 2 \sum_{l=m+1}^L \sigma_l,$$

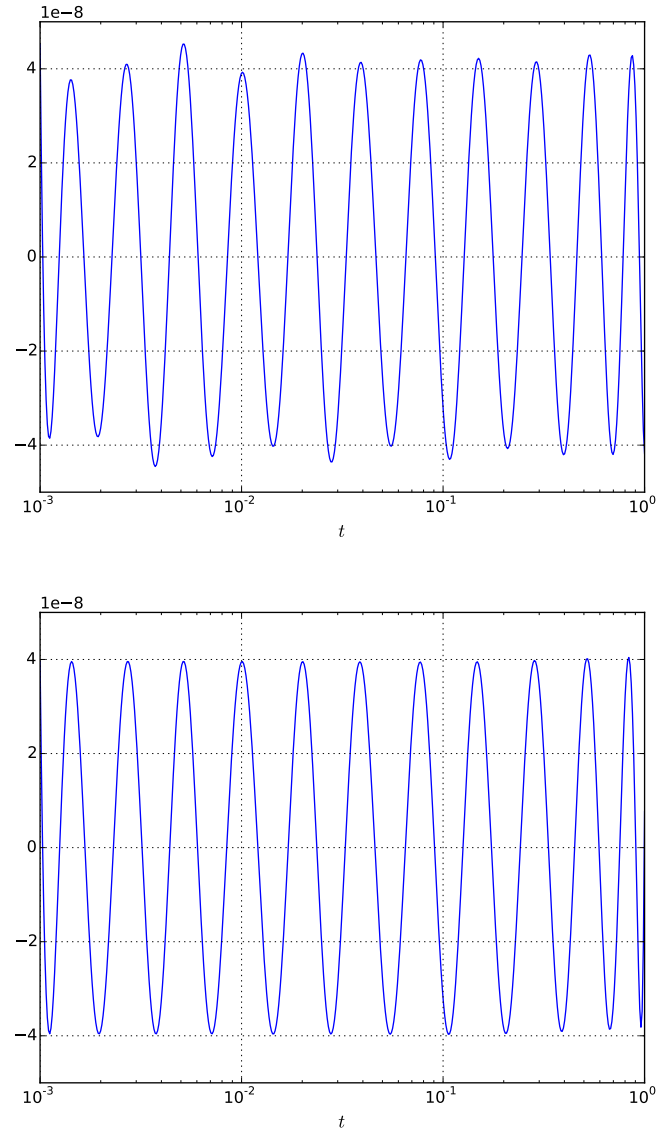
which suggests choosing m such that

$$2(\sigma_{m+1} + \sigma_{m+2} + \cdots + \sigma_N) < \varepsilon. \quad (27)$$

Unfortunately, however, there does not seem to be a simple way to estimate the uniform error $\|g(t) - \hat{g}(t)\|_{L_\infty(\delta, 1)}$.

Example 3. Figure 4 shows the rapid decay of the Hankel singular values for the 42 optimized nodes a_n and weights w_l of Example 2. Shown in blue are the $m = 24$ singular values that we retained when applying the reduction algorithm described above to obtain the nodes \hat{a}_l and \hat{w}_l for $1 \leq l \leq m$. This choice resulted from letting $\varepsilon = 10^{-9}$ in the truncation criterion (27). Figure 5 shows the relative error for the reduced exponential sum, as well as the effect of optimizing the \hat{a}_l and \hat{w}_l using

Fig. 5 Relative error using the 24 nodes \hat{a}_l and weights \hat{w}_l obtained by applying the reduction algorithm, before (top) and after (bottom) optimization.



the algorithm of Section 3. The optimization step leads to a slightly more even distribution of the relative error, but the improvement in the maximum absolute value is not dramatic: from about 4.5×10^{-8} to about 3.9×10^{-8} . We see that both values are little different from the value 4.2×10^{-8} obtained using the unreduced exponential sum, whereas the number of terms has been almost halved, from 42 to 24.

5 Further experiments

We conclude with some further computational experiments that probe how the accuracy of the exponential sum approximation depends on the parameters involved. Also, we give a simple example of the fast algorithm for evaluating fractional integrals that was described in the Introduction.

Table 2 Maximum relative error in reduced exponential sums for three underlying optimized L -term, quadrature approximations using two choices of δ . The errors shown in bold are the smallest for each combination of m and δ . The bottom row shows the errors for the original, unreduced sums.

J, N, N L	$\delta = 10^{-6}$			$\delta = 10^{-9}$		
	25, 4, 4 100	25, 5, 6 149	26, 6, 8 206	35, 4, 4 140	35, 5, 6 209	36, 6, 8 286
$m = 10$	2.24e-01	2.82e-01	3.21e-01	8.82e-01	9.02e-01	9.16e-01
20	1.74e-03	2.11e-03	3.45e-03	1.03e-01	1.10e-01	1.30e-01
30	9.23e-06	1.20e-05	2.41e-05	2.50e-03	2.90e-03	4.59e-03
40	4.64e-08	6.08e-08	1.56e-07	6.16e-05	7.40e-05	1.17e-04
50	1.93e-09	2.77e-10	9.78e-10	1.31e-06	1.61e-06	3.15e-06
60	1.73e-09	6.30e-12	4.48e-12	2.71e-08	3.50e-08	7.65e-08
70				5.34e-09	6.79e-10	1.79e-09
80				4.91e-09	2.50e-11	4.27e-11
	1.73e-09	4.12e-12	8.77e-15	4.90e-09	1.44e-11	2.66e-14

5.1 Dependence on m , δ and L

Table 2 illustrates how the maximum relative error depends on the number m of retained Hankel singular values used to construct a reduced exponential sum, on the choice of δ , and on the number L of terms in the exponential sum obtained by applying the optimization method of Section 3 to the quadrature approximation (18). The bottom row of the table shows the accuracy of this unreduced L -term sum. For $\delta = 10^{-6}$ and $\delta = 10^{-9}$ we used three different choices of L , and then computed the errors for the resulting m -term reduced sums. In this way, for each combination

of m and δ we obtained three different exponential sum approximations based on three different unreduced sums (with three different values for L). The errors shown in bold are the smallest for each combination of m and δ , indicating the best of the three choices of L . The notable feature is that it does not pay to start with a larger L than necessary, most likely due to larger roundoff errors during the computation of the reduced sum.

Table 3 Maximum relative error for different β . In each case, $\delta = 10^{-6}$. The smallest error for each m is shown in bold.

β	0.25	0.50	0.75	1.00	1.50	2.00
L	125	149	149	149	149	180
$m = 30$	1.80e-05	1.20e-05	5.50e-06	9.17e-06	6.59e-04	4.03e-02
40	9.97e-08	6.08e-08	2.70e-08	4.83e-08	3.80e-06	6.17e-04
50	4.22e-10	2.78e-10	1.56e-10	5.52e-10	1.80e-08	4.89e-06
60	4.60e-11	5.12e-12	3.77e-11	3.37e-10	9.31e-10	8.90e-08
	4.49e-11	4.12e-12	3.63e-11	8.06e-11	2.64e-10	3.11e-11

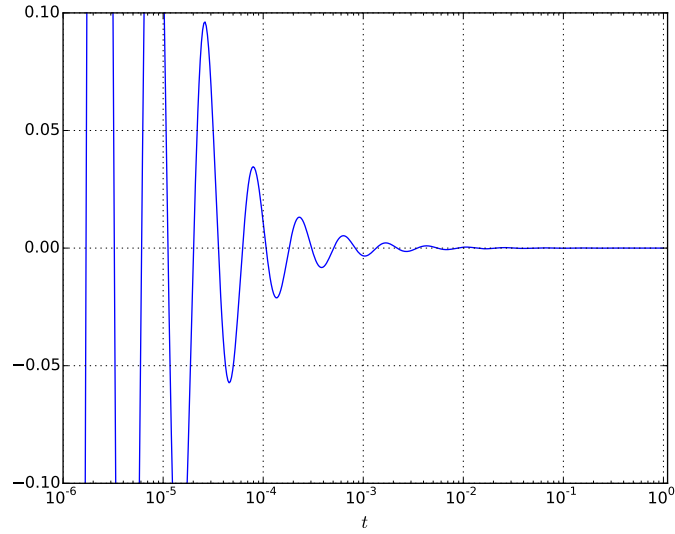
5.2 Dependence on β

Table 3 shows the maximum relative error for six choices of β and four choices of m in the ranges $1/4 \leq \beta \leq 2$ and $30 \leq m \leq 60$. Once again, the bottom row gives the error in the unreduced sum obtained after optimizing the quadrature approximation with L terms. We observe little variation for $1/4 \leq \beta \leq 1$, but as β increases beyond 1, and thus $t^{-\beta}$ becomes more singular, the accuracy for a fixed number of terms m declines noticeably.

Table 4 Maximum absolute errors and convergence rates when evaluating the fractional integral (28) via the fast algorithm based on an exponential sum with $L = 20$ terms. The higher-order scheme used a graded mesh.

N	$U^j = u(t_j)$			$U^j = \frac{1}{2}(u(t_j) + u(t_{j-1}))$		
	e_N	rate	d_N	e_N	rate	d_N
80	1.25e-02		1.49e-06	5.08e-04		1.46e-06
160	6.25e-03	1.0000	1.31e-06	1.80e-04	1.5000	1.76e-06
320	3.13e-03	1.0000	1.57e-06	6.35e-05	1.5000	1.36e-06
640	1.56e-03	1.0000	1.41e-06	2.24e-05	1.5000	1.40e-06
1280	7.81e-04	1.0000	1.43e-06	7.93e-06	1.5000	1.34e-06
2560	3.91e-04	1.0000	1.03e-06	3.40e-06	1.2233	1.50e-06

Fig. 6 Oscillatory behaviour of the exponential sum error (that is, the error itself, not the *relative* error).



5.3 A fractional integral

The fractional integral (4) satisfies the identity

$$I^\alpha \frac{t^\beta}{\Gamma(\beta+1)} = \frac{t^{\beta+\alpha}}{\Gamma(\beta+\alpha+1)}, \quad \text{for } \alpha > 0, \beta > 0 \text{ and } t > 0.$$

Thus, letting

$$u(t) = 1 + \frac{t^{1/2}}{\Gamma(3/2)} = 1 + 2\sqrt{\frac{t}{\pi}}$$

we have

$$I^{1/2}u(t) = \frac{t^{1/2}}{\Gamma(3/2)} + \frac{t}{\Gamma(2)} = 2\sqrt{\frac{t}{\pi}} + t. \quad (28)$$

Also, for $\alpha = 1/2$ the weights (6) can be computed as

$$\omega_{nj} = \frac{2}{\sqrt{\pi}} \frac{\Delta t_j}{\sqrt{t_n - t_{j-1}} + \sqrt{t_n - t_j}} \quad \text{for } 1 \leq j \leq n \leq N.$$

We computed an approximation to $I^{1/2}u(t_n)$ for $0 \leq n \leq N$ using the fast algorithm (8) and (9), based on the same exponential sum with $m = 20$ terms and $\delta = 10^{-6}$,

derived from an unreduced sum with $L = 100$ points, whose maximum relative error is given in Table 2. The left half of Table 4 shows the results obtained using uniform meshes, where

$$e_N = \max_{1 \leq n \leq N} |I_{L,p}^{1/2} U(t_n) - I^{1/2} u(t_n)| \quad \text{and} \quad d_N = \max_{1 \leq n \leq N} |I_{L,p}^{1/2} U(t_n) - I^{1/2} U(t_n)|$$

with $L = 20$ and $p = 1$. Thus, e_N is the maximum absolute error in $I_{L,p}^{1/2} U(t_n)$ whereas d_N is the maximum absolute difference between using the fast method versus direct evaluation of the sum in (5). In other words, e_N is the full discretization error whereas d_N is the error due to the exponential sum approximation alone. Interestingly, d_N is much smaller than the maximum relative error of 1.74×10^{-3} in the exponential sum itself. We see from Figure 6 that the difference between $t^{-1/2}$ and the exponential sum oscillates and decays with increasing t , and is smaller in magnitude than 5×10^{-5} for $0.15 \leq t \leq 1$. Evidently, the oscillations result in some cancellation of errors for small t .

The right half of Table 4 shows the results obtained if we instead define $U^j = \frac{1}{2}(u(t_j) + u(t_{j-1}))$, which is a formally second-order accurate approximation to the value of u at the midpoint of the j th subinterval. Because the integrand of $I^{1/2} u(t)$ is weakly singular, we used a graded mesh $t_n = (n/N)^{3/2}$, but even so could not achieve better than $O(N^{-3/2})$ convergence. Only on the final row, when $N = 2560$, is d_N large enough to have a noticeable effect on e_N .

References

1. Alpert, B., Greengard, L., Hagstrom, T.: Rapid evaluation of nonreflecting boundary kernels for time-domain wave propagation. *SIAM J. Numer. Anal.* **37**, 1138–1164 (2000). DOI 10.1137/S0036142998336916
2. Beylkin, G., Monzón, L.: Approximation by exponential sums revisited. *Appl. Comput. Harmon. Anal.* **28**, 131–149 (2010). DOI 10.1016/j.acha.2009.08.011
3. Braess, D.: *Nonlinear Approximation Theory*. Springer-Verlag (1986)
4. Braess, D., Hackbusch, W.: Approximation of $1/x$ by exponential sums in $[1, \infty)$. *IMA J. Numer. Anal.* **25**, 685–697 (2005). DOI 10.1093/imanum/dri015
5. Glover, K.: All optimal Hankel-norm approximations of linear multivariable systems and their l^∞ -error bounds. *International Journal of Control* **39**, 1115–1193 (1984). DOI 10.1080/00207178408933239
6. Jiang, S., Zhang, J., Zhang, Q., Zhang, Z.: Fast evaluation of the Caputo fractional derivative and its application to fractional diffusion equations. Tech. rep., arXiv:1511.03453v1 (2015)
7. Johnson, S.G.: The NLOpt nonlinear-optimization package (Version 2.4.2). <http://ab-initio.mit.edu/nlopt>
8. Kraft, D.: A software package for sequential quadratic programming. Tech. rep., DFVLR-FB 88-28, Institut für Dynamik der Flugsysteme, Oberpfaffenhofen (1988)
9. Li, J.R.: A fast time stepping method for evaluating fractional integrals. *SIAM J. Sci. Comput.* **31**, 4696–4714 (2010). DOI 10.1137/080736533
10. McLean, W.: Fast summation by interval clustering for an evolution equation with memory. *SIAM J. Sci. Comput.* **34**, A3039–A3056 (2012). DOI 10.1137/120870505
11. Schädle, A., andez, M.L.F., Lubich, C.: Fast and oblivious convolution quadrature. *SIAM J. Sci. Comput.* **28**, 412–438 (2006). DOI 10.1137/050623139

12. von Sydow, B.: Error estimates for Gaussian quadrature formulae. *Numer. Math.* **29**, 59–64 (1977)
13. Xu, K., Jiang, S.: A bootstrap method for sum-of-poles approximations. *J. Sci. Comput.* **55**, 16–39 (2013). DOI 10.1007/s10915-012-9620-9